Wastewater Treatment System Optimization for Sustainable Operation of the SHARON–Anammox Process under Varying Carbon/Nitrogen Loadings

Paulina Vilela [1,*], Kijeon Nam [2] and Changkyoo Yoo [2,*]

Supplementary Materials

Number of pages: 25

Number of tables: 9

Number of figures: 5

Table of Contents

1. Methods

1.1. BSM2-SHAMX model

The influent flowrate and concentrations utilized in the BSM2-SHAMX model are presented in Figure S1. The plant's design is adapted from Alex et al. [1] and Volcke et al. [2]. The plant is composed by a primary clarifier with a volume of 900 m^3, five biological reactors with a volume of 1500 m^3 each non-aerated reactor and 3000 m^3 each aerated reactor, secondary clarifier with a volume of 6000 m^3, a thickener, anaerobic digester, dewatering unit [1], followed by the SHARON reactor with a volume of 338 m^3 and Anammox reactor with a volume of 75 m^3 [2]. The model uses an average influent dry-weather flow rate of 20,648.36 m^3/d, average biodegradable COD in the influent concentration of 592.53 g/m^3 [1]. The SHARON reactor is developed as a continuously stirred tank reactor (CSTR), with a hydraulic retention time (HRT) of 24 hours [2], while the HRT off the BMS2 model is 22 hours based on the influent flowrate and total reactors volume [1]. The plant model configuration presented in this study is shown in Figure S2.

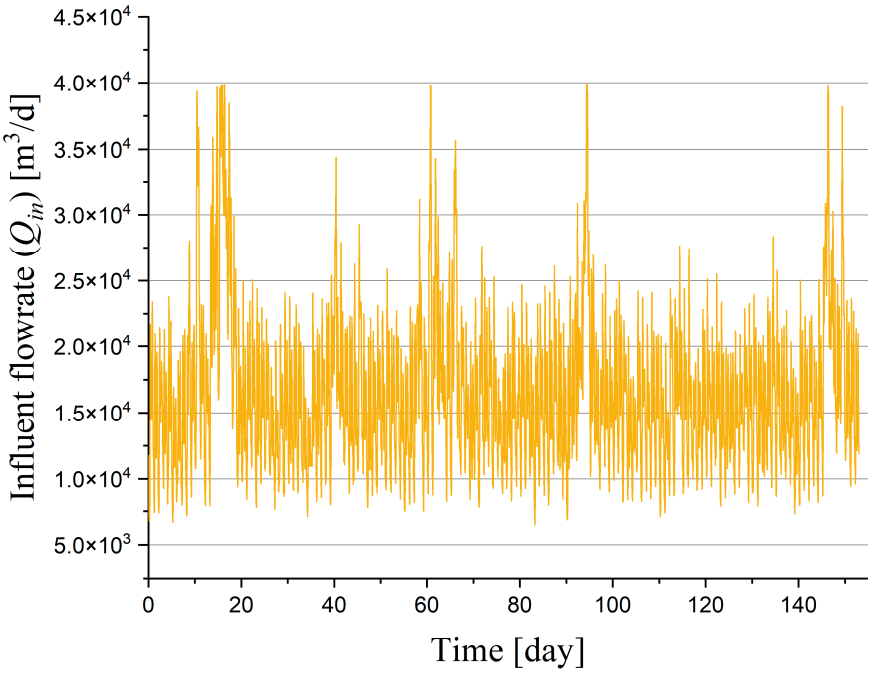
Influent flowrate (Q_{in}) [m^3/d]
4.5×10^4
4.0×10^4
3.5×10^4
3.0×10^4
2.5×10^4
2.0×10^4
1.5×10^4
1.0×10^4
5.0×10^3
0
20
40
60
80
100
120
140
Time [day]

(a)

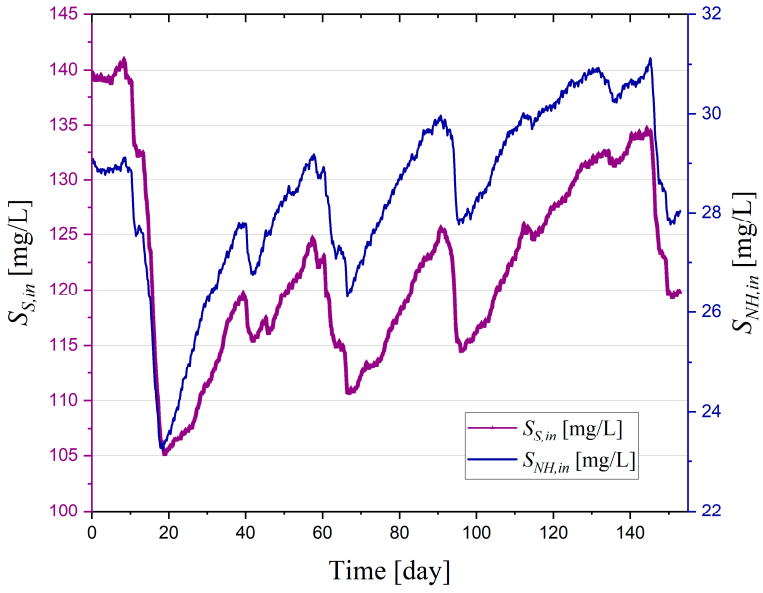
$S_{S,in}$ [mg/L]
$S_{NH,in}$ [mg/L]
145
140
135
130
125
120
115
110
105
100
32
30
28
26
24
22
0
20
40
60
80
100
120
140
Time [day]
$S_{S,in}$ [mg/L]
$S_{NH,in}$ [mg/L]

(b)

Figure S1. Long term influent profiles for the BSM2-SHAMX model. (a) Influent flowrate profile for a 153d operation horizon. (b) Influent concentrations profile for a 153d operation horizon.

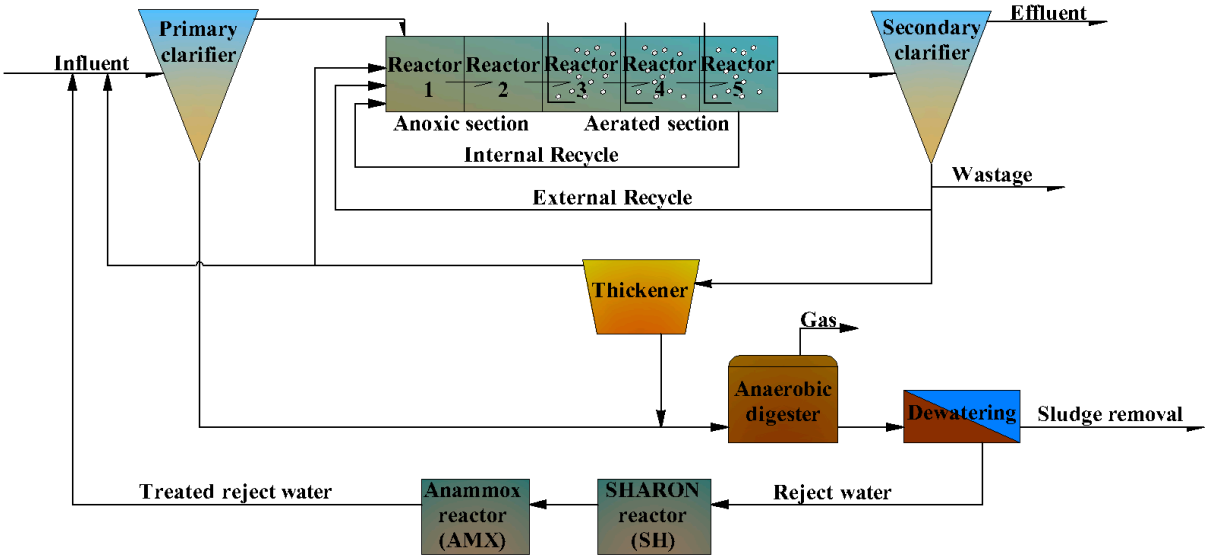

Figure S2. BSM2-SHAMX plant configuration represented in Simulink-MATLAB.

1.1.1. Benchmark simulation model No. 2

The Benchmark Simulation Model No. 2 (BSM2) is a wastewater modeling methodology that portrays a common layout of a real wastewater treatment plant (WWTP) [3]. BSM2 configuration encloses an environment for simulation, influent loadings, test procedure, and evaluation criteria [3,4]. These variables guide most of the reactions and rate coefficients occurring in the treatment system presenting variations for the factors of plant configuration, operating conditions, microorganism population dynamics, composition of the influent wastewater load, pH, among others. Thus, several simplifications and assumptions were made for the BSM2 modeling, in both physical and mathematical model structure. The pH being one of the most important was considered to remain constant, and by restriction of the mathematical model it was controlled by the

alkalinity measure (S_{alk}) [3]. In addition, the influent data of the WWTP from the International Water Association (IWA) Task Group report of the BSM2 groups static and dynamic seven-day data for three weather conditions: storm, rain, and dry conditions [3,5].

1.1.2. Stoichiometries and kinetics of BSM2-SHAMX

Table S1. Model components of ASM1 at BSM2 [3,6].

No.	State variables (components)	Symbol	Unit
1	Soluble undegradable organics	S_I	mg COD/L
2	Soluble biodegradable organics	S_S	mg COD/L
3	Particulate undegradable organics	X_I	mg COD/L
4	Particulate biodegradable organics	X_S	mg COD/L
5	Active heterotrophic biomass	X_{BH}	mg COD/L
6	Active autotrophic biomass	X_{BA}	mg COD/L
7	Particulate undegradable endogenous products	X_P	mg COD/L
8	Dissolved oxygen	S_O	mg COD/L
9	Nitrate and nitrite (NO_3 + NO_2)	S_{NO}	mg N/L
10	Ammonia (NH_4 + NH_3)	S_{NH}	mg N/L
11	Soluble biodegradable organic N	S_{ND}	mg N/L
12	Particulate biodegradable organic N	X_{ND}	mg N/L
13	Alkalinity	S_{ALK}	mol HCO_3^-/m^3
14	Total suspended solids	*TSS*	mg TSS/L
15	Flowrate	*Q*	mg/L

Table S2. Model components of SHARON process at BSM2-SHAMX. Adapted from [2].

No.	State variables (components)	Symbol	Unit
1	Total ammonium	S_{NH}	mole/m^3
2	Total nitrite	TNO_2	mole/m^3
3	Total inorganic carbon	*TIC*	mole/m^3
4	Total inorganic phosphorus	*TIP*	mole/m^3

5	Total nitrate	S_{NO}	mole/m^3
6	Dissolved oxygen	S_O	mole/m^3
7	Nitrogen gas	N_2	mole/m^3
8	Ammonium oxidizing biomass	X_{NH}	mole/m^3
9	Nitrite oxidizing biomass	X_{NO2}	mole/m^3
10	Heterotrophic biomass	X_{bh}	mole/m^3
11	Methanol	CH_3OH	mole/m^3
12	Protons	H^+	mole/m^3

Table S3. Model components of Anammox process at BSM2-SHAMX. Adapted from [2].

No.	State variables (components)	Symbol	Unit
1	Dissolved oxygen	S_O	gO$_2$/m^3
2	Readily biodegrtadable substrate	S_S	gCOD/m^3
3	Total ammonium	S_{NH}	gN/m^3
4	Total nitrite	TNO_2	gN/m^3
5	Total nitrate	TNO_3	gN/m^3
6	Nitrogen gas	N_2	gN/m^3
7	Heterotrophic biomass	X_{bh}	gCOD/m^3
8	Ammonium oxidizing biomass	X_{NH}	gCOD/m^3
9	Nitrite oxidizing biomass	X_{NO2}	gCOD/m^3
10	Anammox biomass	X_{AN}	gCOD/m^3
11	Slowly biodegradable substrate	X_S	gCOD/m^3
12	Particulate products from biomass decay	X_P	gCOD/m^3
13	Alkalinity	S_{alk}	mole/m^3

Table S4. Kinetic parameter values of SHARON and Anammox in the BSM2-SHAMX model. Adapted from [2].

Parameter	Symbol	Value at 35°C	Unit	Reference
Maximum growth rate ammonia oxidizers	μ_{max}^{nh}	2.1	1/d	[2]

Ammonia substrate saturation for ammonia oxdizers	$K_{NH_3}^{nh}$	0.054	mole/m^3	[2,7,8]
Oxygen substrate saturation for ammonia oxidizers	K_{i,TNO_2}^{nh}	0.029	mole/m^3	[2,7,8]
Maximum growth rate nitrite oxidizers	μ_{max}^{nit}	0.146	1/d	[2]
Nitrous acid substrate saturation for nitrite oxidizers	$K_{TNO_2}^{nit}$	1.05	mole/m^3	[2,7,8]
Oxygen substrate saturation for nitrite oxidizers	$K_{S_O}^{nit}$	0.019	mole/m^3	[2,7,8]
Maximum growth rate nitrite denitrifiers	$\mu_{max}^{dTNO_2}$	0.034	1/d	[2]
Nitrite substrate saturation for nitrite denitrifiers	$K_{TNO_2}^{dTNO_2}$	0.009	mole/m^3	[2,7,8]
Methanol substrate saturation during denitrification	$K_{CH_3OH}^{bh,an}$	0.52	mole/m^3	[2,7,8]
Oxygen 'inhibition constant' for denitrifiers	K_{i,S_O}	0.006	mole/m^3	[2,7,8]
Maximum growth rate nitrate denitrifiers	$\mu_{max}^{dS_{NO}}$	1.5	1/d	[2]
Nitrate substrate saturation for nitrate denitrifiers	$K_{S_{NO}}^{dS_{NO}}$	0.01	mole/m^3	[2,7,8]
Maximum growth rate methanol oxidizers	$\mu_{max}^{CH_3OH}$	2.5	1/d	[2]
Methanol substrate saturation during aerobic growth	$K_{CH_3OH}^{bh,aer}$	2.08	mole/m^3	[2,7,8]
Oxygen substrate saturation for methanol oxidizers	$K_{S_O}^{bh}$	0.0025	mole/m^3	[2,7,8]

Maximum growth rate ammonia oxidizers	μ_{max}^{nh}	2.1	1/d	[2]

Table S5. Petersen matrix of the ASM1 model. Adapted from [2].

No.	State variables (components)	Symbol	Components transformations												
			S_O	S_{NH}	S_{NO}	X_{bh}	X_{ba} *to AOB and NOB*	S_S *to* CH_3OH	X_S *to* CH_3OH	S_{ND} *to* S_{NH}	X_{ND} *to* S_{NH}	S_I	X_I	X_P	S_{alk} *to TIC*
1	Soluble inert organic matter	S_I	0	0	0	0	0	0	0	0	0	**-1**	0	0	0
2	Readily biodegradable substrate	S_S	0	0	0	0	0	0	0	0	0	0	**-1**	0	0
3	Particulate inert organic matter	X_I	0	0	0	0	0	**-1**	0	0	0	0	0	0	0
4	Slowly biodegradable substrate	X_S	0	0	0	0	0	0	**-1**	0	0	0	0	0	0
5	Active heterotrophic biomass	X_{bh}	0	0	0	**-34.58**	0	0	0	0	0	0	0	0	0
6	Active autotrophic biomass	X_{ba}	0	0	0	0	**-34.58**	0	0	0	0	0	0	0	0
7	Particulate products arising from biomass decay	X_P	0	0	0	0	0	0	0	0	0	0	0	**-1**	0
8	Oxygen	S_O	**-32**	0	0	0	0	0	0	0	0	0	0	0	0
9	Nitrate and nitrite nitrogen	S_{NO}	0	0	**-14**	0	0	0	0	0	0	0	0	0	0

10	$NH4^+ + NH3$ nitrogen	S_{NH}	0	**-14**	0	**-0.02**	**-0.02**	**-0.05**	**-0.05**	0	0	0	0	0	0
11	Soluble biodegradable organic nitrogen	S_{ND}	0	0	0	0	0	0	0	**-14**	0	0	0	0	0
12	Particulate biodegradable organic nitrogen	X_{ND}	0	0	0	0	0	0	0	0	**-14**	0	0	0	0
13	Alkalinity	S_{alk}	0	0	0	**0.05**	**0.05**	**-0.0002**	**-0.0002**	0	0	0	0	0	**-1**

Table S6. Petersen matrix of the of the SHARON model. Adapted from [2].

No.	State variables (components)	Symbol	Components transformations											
			S_{NH}	TNO_2	S_{NO}	S_O	X_{NH}	X_{NO2}	X_{bh}	CH_3OH to S_S	S_I	X_I	X_P	TIC to S_{alk}
1	Total ammonium	S_{NH}	**-1**	0	0	0	0	0	0	0	0	0	0	0
2	Total nitrite	TNO_2	0	**-1**	0	0	0	0	0	0	0	0	0	0
3	Total inorganic carbon	TIC	0	0	0	0	0	0	0	0	0	0	0	**-1**
4	Total nitrate	S_{NO}	0	0	**-1**	0	0	0	0	0	0	0	0	0
5	Dissolved oxygen	S_O	0	0	0	**-1**	0	0	0	0	0	0	0	0
6	Ammonium oxidizing biomass	X_{NH}	0	0	0	0	**-1**	0	0	0	0	0	0	0
7	Nitrite oxidizing biomass	X_{NO2}	0	0	0	0	0	**-1**	0	0	0	0	0	0
8	Heterotrophic biomass	X_{bh}	0	0	0	0	0	0	**-1**	**-0.02**	0	0	0	0
9	Methanol	CH_3OH	0	0	0	0	0	0	0	**-0.009**	0	0	0	0
10	Soluble inert organic matter	S_I	0	0	0	0	0	0	0	0	**-1**	0	0	0
11	Particulate inert organic matter	X_I	0	0	0	0	0	0	0	0	0	**-1**	0	0

12	Particulate products arising from biomass decay	X_P	0	0	0	0	0	0	0	0	0	0	**-1**	0

Table S7. Petersen matrix of the Anammox model. Adapted from [2].

No.	State variables (components)	Symbol	Components transformations														
			S_O	S_S	S_{NH}	N_2	X_{bh}	X_S	X_P	S_{NO}	TNO_2	X_{NH} to X_S	X_{NO_2} to X_S	X_{AN} to X_S	S_I	X_I	S_{alk}
1	Oxygen	S_O	**-1**	0	0	0	0	0	0	0	0	0	0	0	0	0	0
2	Readily biodegradable substrate	S_S	0	**-1**	0	0	0	0	0	0	0	0	0	0	0	0	0
3	$NH4^+$ + NH3 nitrogen	S_{NH}	0	0	**-1**	0	0	0	0	0	0	0	0	0	0	0	0
4	Total nitrite	TNO_2	0	0	0	0	0	0	0	0	**-1**	0	0	0	0	0	0
5	Total nitrate	S_{NO}	0	0	0	0	0	0	0	**-1**	0	0	0	0	0	0	0
6	Nitrogen gas	N_2	0	0	0	**-1**	0	0	0	0	0	0	0	0	0	0	0
7	Active heterotrophic biomass	X_{bh}	0	0	0	0	**-1**	0	0	0	0	0	0	0	0	0	0
8	Ammonium oxidizing biomass	X_{NH}	0	0	0	0	0	0	0	0	0	**-1**	0	0	0	0	0
9	Nitrite oxidizing biomass	X_{NO2}	0	0	0	0	0	0	0	0	0	0	**-1**	0	0	0	0
10	Anammox biomass	X_{AN}	0	0	0	0	0	0	0	0	0	0	0	**-1**	0	0	0
11	Slowly biodegradable substrate	X_S	0	0	0	0	0	**-1**	0	0	0	0	0	0	0	0	0
12	Particulate products arising from biomass decay	X_P	0	0	0	0	0	0	**-1**	0	0	0	0	0	0	0	0
13	Alkalinity	S_{alk}	0	0	0	0	0	0	0	0	0	0	0	0	0	0	**-1**
14	Soluble inert organic matter	S_I	0	0	0	0	0	0	0	0	0	0	0	0	**-1**	0	0
15	Particulate inert organic matter	X_I	0	0	0	0	0	0	0	0	0	0	0	0	0	**-1**	0

1.2. SHARON and Anammox model calibration

In the model calibration, the parameters into the model can be tuned to best follow experimental data. For calibration, the data for the model-based WWTP was obtained from literature [3,9–13], where each process data was adapted to the SHAMX in the model. The conditions of each study are analyzed to apply to the SHAMX model presented in this study. Next, a deduction of the model parameters is done to fit the experimental data to the model by using the genetic algorithm and bounds of parameters from literature (Table S8). Finally, to verify the parameters' calibration it is needed to calculate the error between the simulated and experimental values obtained. In this study, there sum of squared errors (SSE) and the root mean square error (RMSE) are calculated [5,14].

Table S8. Kinetic parameter value ranges for calibration of ASM model in BSM2-SHAMX.

Parameter	Symbol	Value	Value range	Reference
Maximum growth rate of heterotrophic biomass	μ_H	1.00	0.90 – 1.10	[9]
Saturation coefficient for organic matter	K_S	3.00	2.70 – 3.30	
Heterotrophic saturation coefficient for oxygen	K_{OH}	0.20	1.80 – 0.22	[3,10]
Saturation coefficient for nitrate	K_{NO}	0.50	0.45 – 0.55	[9]
Heterotrophic decay rate	b_h	0.05	0.045 – 0.055	[9,13]
Maximum growth rate of autotrophic biomass	μ_A	0.50	0.45 – 0.55	[3,10]

Saturation coefficient for ammonia	K_{NH}	0.01	0.009 – 0.011	[9,13]
Autotrophic saturation coefficient for oxygen	$K_{O,A}$	0.50	0.45 – 0.55	[9]
Autotrophic decay rate	b_A	0.05	0.045 – 0.55	[3,10]
Correction factor for anoxic hydrolysis	η_g	0.80	0.72 – 0.88	
Ammonification coefficient	k_a	2.00	1.80 – 2.20	
Hydrolysis rate	k_h	3.00	2.70 – 3.30	[9]
Hydrolysis constant	K_X	1.00	0.90 – 1.10	
Heterotrophic yield coefficient	Y_H	0.74	0.67 – 0.81	
Autotrophic yield coefficient	Y_A	0.24	0.216 – 0.264	[3,10,11]
Fraction of inert product by biomass	f_P	0.20	0.18 – 0.22	[11]
Ammonia fraction in biomass	i_{XB}	0.08	0.072 – 0.088	[3,10,12]
Ammonia fraction in particulate products	i_{XP}	0.06	0.054 – 0.066	

Table S9. Calibrated kinetic parameters of ASM model in BSM2-SHAMX.

	Kinetic parameter	Default		Calibrated value
		Value	Reference	
COD	μ_H	1.00	[9]	0.5377
	$K_{O,A}$	0.50		1.00
	η_g	0.80	[3]	0.05
TN	μ_H	1.00	[9]	0.50
	K_{NH}	0.01	[9,13]	0.05
	K_X	1.00	[9]	0.0109
	η_g	0.80	[3]	0.05
	Y_A	0.24	[3,11]	1.00

1.3. Control performance assessment

Control performance provides information related to the good performance of the implemented controller. This analysis is divided into two levels. The first level deals with the analysis of effluent quality and further operational cost. The second level refers to an assessment of the local control loops and helps to provide measures of the effect of the control strategies on the plant performance [15].

1.3.1. First level assessment

The performance index is a set of geographically independent measures including an effluent quality measure, energy required for pumping and aeration, and sludge production [3,16]. The effluent quality index (EQI) quantifies the effluent pollution load that discharges to a water body. The following methodology was developed by [15] and is represented in Equation S1.

$$EQI = \frac{1}{1000(t_f - t_0)} \int_{t_0}^{t_f} \begin{pmatrix} \beta_{TSS} TSS_e(t) + \beta_{COD} COD_e(t) + \beta_{BOD} BOD_e(t) + \\ \beta_{TKN} TKN_e(t) + \beta_{NO} NO_e(t) \end{pmatrix} Q_e(t) dt \quad \text{(S1)}$$

where TSS_e is the total suspended solids concentration in the effluent, COD_e is the chemical oxygen demand concentration in the effluent, BOD_e is the biological oxygen demand concentration in the effluent, TKN_e is the total Kjeldahl nitrogen, and NO_e is the total nitrogen concentration in the effluent. β_{TSS} , β_{COD} , β_{BOD} , β_{TKN} , and β_{NO} are the component weighting values, which have the value of 2, 1, 2, 20, and 20, respectively. The weights were taken from [15] based on the Flanders effluent quality formula for calculations of fines. t_f and t_0 represent the starting and ending time of the evaluation, respectively, and Q_e is the effluent flowrate.

1.3.2 Second level assessment

The second level is divided into two sub-levels to assess the controlled variable performance and the manipulated variable performance.

1.3.2.1 Controlled variable performance

The error presented in the model is calculated using Equation S2 to Equation S7 [3].

$$IAE_i = \int_{t_0}^{t_f} |e_j| dt \tag{S2}$$

$$ISE_j = \int_{t_0}^{t_f} e_j^2 dt \tag{S3}$$

$$\max(Dev_j^{error}) = \max|e_j| \tag{S4}$$

$$Var(e_j) = \overline{e_j^2} - (\overline{e_j})^2 \tag{S5}$$

$$\overline{e_j} = \frac{\int_{t_0}^{t_f} e_j dt}{t_f - t_0} \tag{S6}$$

$$\overline{e_j^2} = \frac{\int_{t_0}^{t_f} e_j^2 dt}{t_f - t_0} \tag{S7}$$

Here, IAE_i is the integral of the absolute error, ISE_j is the integral of the squared error, $\max(Dev_j^{error})$ is the maximum deviation from setpoint, $Var(e_j)$ is the variance in the controlled variable error, e_j is the error in the controlled variable and is calculated using Equation S8.

$$e_j = Z_{j,setpoint} - Z_{j,observed} \tag{S8}$$

Here, $Z_{j,setpoint}$ is the setpoint value established for the control, and $Z_{j,observed}$ is the measured value of the controlled variable.

1.3.2.2 Manipulated variable performance

The error presented in the simulations in the model is calculated using Equation S9 to Equation S14 [3].

$$\max(Dev_j^{MV}) = u_{j,\max} - u_{j,\min} \tag{S9}$$

$$\max(Dev_j^{\Delta u_j}) = \max(\Delta u_j) \tag{S10}$$

$$Var(\Delta u_j) = \overline{\Delta u_j^2} - (\overline{\Delta u_j})^2 \tag{S11}$$

$$\overline{\Delta u_j} = \frac{\int_{t_0}^{t_f} \Delta u_j dt}{t_f - t_0} \tag{S12}$$

$$\overline{\Delta u_j^2} = \frac{\int_{t_0}^{t_f} \Delta u_j^2 dt}{t_f - t_0} \tag{S13}$$

Here, $\max(Dev_j^{MV})$ is the maximum deviation in the manipulated variable (MV), $\max(Dev_j^{\Delta u_j})$ is the maximum deviation in the change in the manipulated variable, $Var(\Delta u_j)$ is the variance in the change in the manipulated variable, u_j is the value of the manipulated variable, and $\overline{\Delta u_j}$ is calculated using Equation S19.

$$\Delta u_j = \left| u_j(t+dt) - u_j(t) \right| \tag{S14}$$

1.3.3 Operational cost

The operational cost is evaluated using aeration energy (AE), pumping energy (PE), sludge production (SP), and methane production (METP). Equation S15 to Equation S18 are used to estimate the operational cost index (OC), which was adopted from [3].

$$OC = \gamma_1 AE + \gamma_1 PE + \gamma_2 SP \tag{S15}$$

Here, γ_1, and γ_2 have values of 0.1 €/kWh [17,18], and 0.16 €/kg [18].

$$AE = \frac{S_O^{sat}}{1.8(1000)(t_f - t_0)} \int_{t_0}^{t_f} \sum_{i=1}^{5} V_i (K_{Lai})(t) dt \tag{S16}$$

Here, S_O^{sat} is 8 mg/L, and V_i is the volume of the reactor.

$$PE = \frac{1}{t_f - t_0} \int_{t_0}^{t_f} (0.004 Q_{ir}(t) + 0.008 Q_r(t) + 0.05 Q_W(t)) dt \tag{S17}$$

Here, Q_{ir} is the internal recycle flowrate, Q_r is the return sludge flowrate, and Q_W is the wastage flowrate.

$$SP = \frac{1}{t_f - t_0} \left(TSS_f - TSS_0 + 0.75 \left(\int_{t_0}^{t_f} (X_{S,e} + X_{I,e} + X_{B,H,e} + X_{B,A,e})(Q_e)(t) dt \right) \right) \tag{S18}$$

Here, $X_{S,e}$ represents the parameter of particulate biodegradable organics in the effluent flow, $X_{I,e}$ is the particulate undegradable organics, $X_{B,H,e}$ is the active heterotrophic biomass, and $X_{B,A,e}$ is the active autotrophic biomass.

$$METP = \frac{16(P_{atm})(13.89)}{25.62(t_f - t_0)} \left(\int_{t_0}^{t_f} \frac{Q_{gas}(t) \cdot p_{gas,CH_4}(t)}{P_{gas}(t)} dt \right) \tag{S19}$$

Here, P_{atm} represents the atmospheric pressure with a value of 1.013, Q_{gas} is the methane gas (CH_4) flowrate, p_{gas,CH_4} is the methane gas pressure, and P_{gas} is the gas pressure considering CO_2, H_2, and H_2O.

1.4. Sensitivity analysis

Sensitivity analysis methods are classified in mathematical, statistical, and graphical. Mathematical sensitivity analysis assesses the output of a model to an input parameter with a variation range [19]. In the sensitivity analysis, the result shows a sensitivity ranking of the input parameters reflecting their influence on the model output [20]. Furthermore, scatter plots showing the input parameters versus the model output are utilized to represent the degree of correlation and linearity of the relationship between the input and output [20]. In the scatter plots, the metrics of rank correlation (Spearman's ρ), rank partial correlation, and the rank standardized regression, are represented in a scale of -1 to 1. The rank correlation indicates the level of monotonicity between the input and output values of the samples and can be calculated using the Equation (S20) for Pearson correlation using rank transformed data, with linearized monotonic nonlinear relation between the variables [21].

$$\rho(a,b) = \frac{E(ab)}{\sigma_a \sigma_b} \tag{S20}$$

where ρ is the Pearson correlation coefficient, a and b are two zero-mean real-valued random variables, $E(ab)$ is the cross-correlation of a and b, and $\sigma_a \sigma_b$ are calculated from the variances of a and b, where $\sigma_a^2 = E(a^2)$ and $\sigma_b^2 = E(b^2)$. Moreover, the rank partial correlation indicates the correlation between other input variables. Equation (S21) shows the calculation of the partial correlation coefficient [20].

$$r_{X_1Y|X_2} = \frac{r_{X_1Y} - r_{X_1X_2} r_{X_2Y}}{\sqrt{\left(1-r^2_{X_1X_2}\right)\left(1-r^2_{X_2Y}\right)}} \quad \text{(S21)}$$

where X_1 and X_2 are the input parameters, Y is the model output, $r_{X_1Y|X_2}$ is the partial correlation coefficient for X_1 and Y based on the effect of X_2. Moreover, the rank partial correlation indicates the correlation between other input variables. In addition, the rank standardized regression is derived from the rank regression, which utilizes matrix techniques to calculate the regression coefficients where the sensitivity of the parameters is evaluated in the regression equation. Monte Carlo simulation linear regression is commonly used to analyze the uncertainty of model outputs. The model structure is represented by *f*, state variables as *x*, input variables as u, parameters by *P*, and output vectors as *y* (Equation S22 to Equation S26) [22]. In the present study, the given variability of the input parameters is generated and implemented with MATLAB R2016a/Simulink.

$$\frac{dx}{dt} = f(x,u,t,P) \quad \text{(S22)}$$

$$x(t_0) = x_0 \quad \text{(S23)}$$

$$y = g(x(t)) \quad \text{(S24)}$$

This methodology consisted of the following steps: (a) specify input uncertainty, (b) sample input uncertainty, (c) run the simulation and, (d) use the sampling matrix θ_i. Equation S25 and Equation S26 show the theoretical output regression from Monte Carlo simulations and its standardized coefficients β_i.

$$y_{reg} = a + \sum_i b_i \theta_i \quad \text{(S25)}$$

$$\beta_i = \frac{\sigma_{\theta_i}}{\sigma_y} b_i \quad \text{(S26)}$$

Here, b_i are the regression coefficients scaled with the standard deviation of the model input and output. The sensitivity coefficient b_i indicates a large effect of the corresponding output parameter in the regression when it takes a high absolute value; when the value is negative and positive, it represents a negative effect, and positive effect, respectively. However, when the value is zero, the output is not sensitive to the parameter, presenting a negligible relationship [22].

Thus, the rank standardized regression removes the influence of the different units of the parameters, placing them on the same level. Equation (S27) shows the calculation of the rank standardized regression.

$$\left(\frac{\hat{Y}-\overline{Y}}{s}\right)=\sum_{k}\left[\frac{b_k s_k}{s}\right]\left(\frac{\left(Z_k-\overline{Z}_k\right)}{s_k}\right) \quad \text{(S27)}$$

where Z_k ais a function of the input parameters $X_1,\ldots, X_n$, s is the standardized deviation of Y, and s_k is the standard deviation of the input parameters. In general, both the rank regression and the rank standardized regression are similar exhibiting the same type of sensitivity ranking in numerical values [20].

1.5. Controllers

Process control is the methodology for constraining the process output by manipulating a chosen variable [23]. Proportional-Integrative-Derivative (PID) controllers (Figure S1) are commonly used in industrial processes, and are structured as shown Equation S28 to Equation S31:

$$u_p(t)=k_c(y_s(t)-y(t)) \quad \text{(S28)}$$

$$u_I(t)=\frac{k_c}{\tau_i}\int_0^t(y_s(\tau)-y(\tau))d\tau \quad \text{(S29)}$$

$$u_D(t)=k_c\tau_d\frac{d(y_s(t)-y(t))}{dt} \quad \text{(S30)}$$

Here, $y_s(t)$ represents the setpoint, $y(t)$ is the process output, k_c is the proportional gain, τ_i is the integral time, τ_d is the derivative time. $u_p(t)$, $u_I(t)$, $u_D(t)$ are considered in the PID controller general equation:

$$u(t) = u_p(t) + u_I(t) + u_D(t) \tag{S31}$$

where $u(t)$ is the control output. System identification is necessary for controllers since the process output may deviate from the normal steady state with the open loop identification method. The system identification may be carried out with a signal test like a simple set point change in PID or a step response, as is utilized in this study. First, the process is activated (process input and output present the required information). Second, the integral transform is used to convert the parametric differential equation. Finally, a least square method is used for estimating model parameters from the measured process data [23]. A mathematical representation of the transfer function of the process may be defined as in Equation S32:

$$Gp(s) = \frac{y(s)}{u(s)} = \frac{b_m s^m + b_{m-1} s^{m-1} + \ldots + b_1 s + b_0}{a_n s^n + a_{n-1} s^{n-1} + \ldots + a_1 s + 1} \tag{S32}$$

where $Gp(s)$ represents the transfer function of the process, $y(s)$ is the process output, $u(s)$ is the Laplace transform of the process input (controller output), and $m \leq n$. Then, the process model is tunned with the Ziegler-Nichols method [23]. The software utilized for simulating this control model is MATLAB R2016a/Simulink, which is a block diagram environment integrated in MATLAB that supports simulation and code generation among other functionalities.

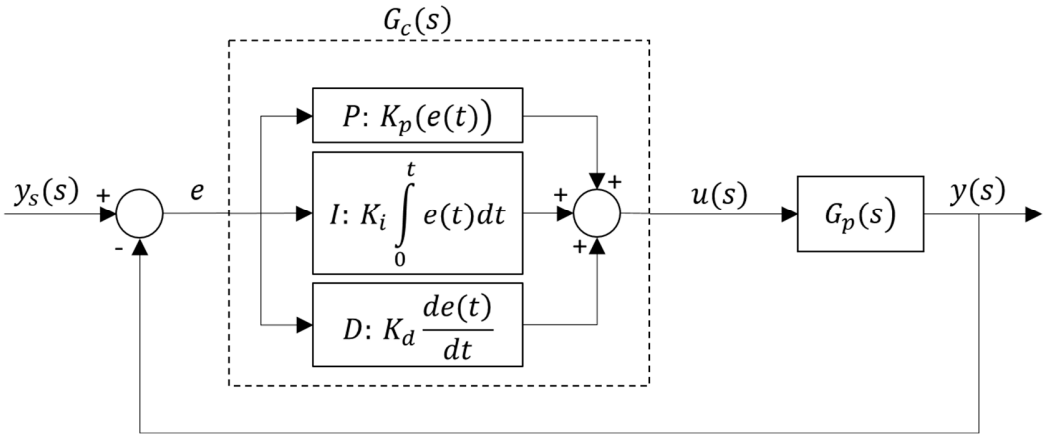

Figure S3. General layout of a PID controller [5].

1.5.1. Model predictive control

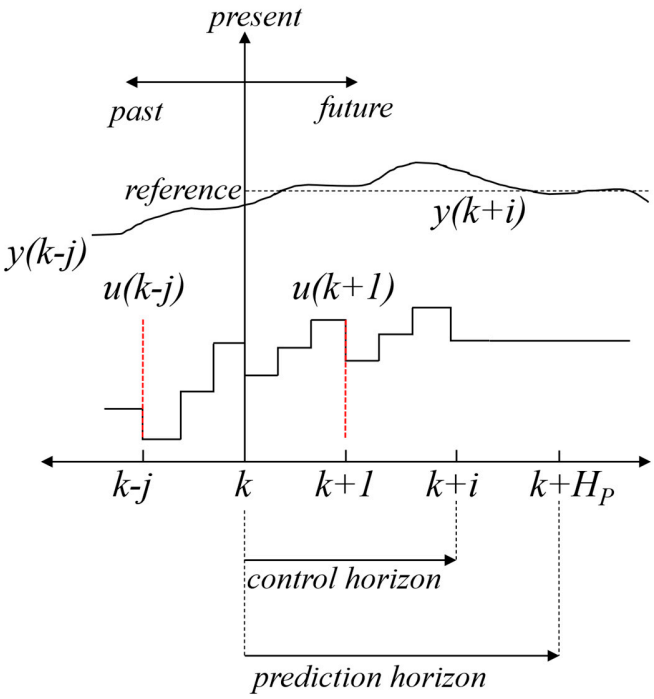

Figure S4. Receding horizon principle of MPC. Adapted from [24,25].

1.5.2. Control strategy scenarios C1 and C2

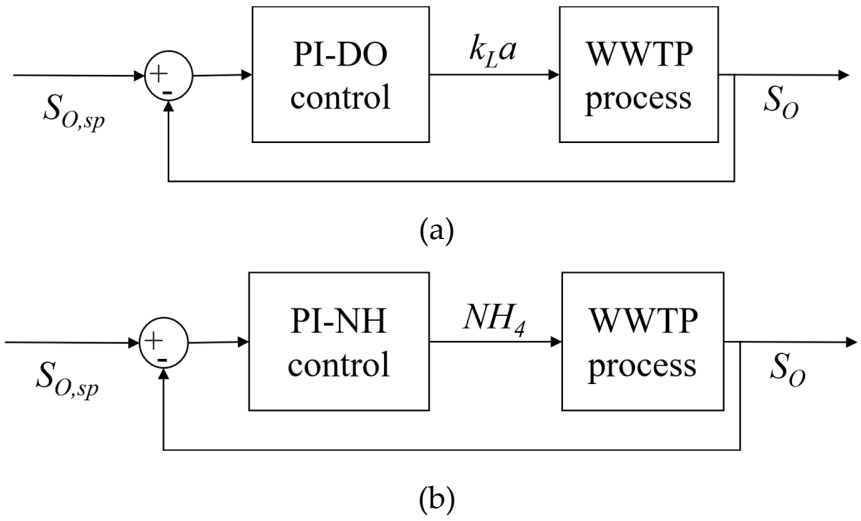

Figure S5. Block diagram of the proposed single loop control strategy (scenario C1 and C2). (a) The control loop calculates the dissolved oxygen concentration (S_O) at the set point given $S_{O,sp}$, and tracks the S_O set point by adjusting the k_La of the system. (b) The control loop compensates the errors of SO measurement to attain to the desired NO_2/NH_4 ratio.

References

1. Alex, J.; Beteau, J.F.; Copp, J.B.; Hellinga, C.; Jeppsson, U.; Marsili-Libelli, S.; Pons, M.N.; Spanjers, H.; Vanhooren, H. Benchmark for Evaluating Control Strategies in Wastewater Treatment Plants. *Eur. Control Conf. ECC 1999 - Conf. Proc.* **2015**, 3746–3751.
2. Volcke, E.I.P.; Vanrolleghem, P.; van Loosdrecht, M.C.M. Modelling, Analysis and Control of Partial Nitritation in a SHARON Reactor, 2006.
3. Alex, J.; Benedetti, L.; Copp, J.; Gernaey, K. V; Jeppsson, U.; Nopens, I.; Pons, M.; Rieger, L.; Rosen, C.; Steyer, J.P.; et al. *Benchmark Simulation Model No. 2 (BSM2) Report*; 2008;
4. Jeppsson, U.; Pons, M.N. The COST Benchmark Simulation Model-Current State and Future Perspective. *Control Eng. Pract.* **2004**, *12*, 299–304, doi:10.1016/j.conengprac.2003.07.001.

5. Vilela, P.; Liu, H.; Lee, S.; Hwangbo, S.; Nam, K.; Yoo, C. A Systematic Approach of Removal Mechanisms, Control and Optimization of Silver Nanoparticle in Wastewater Treatment Plants. *Sci. Total Environ.* **2018**, *633*, doi:10.1016/j.scitotenv.2018.03.247.

6. Henze, M.; Grady, C.; Gujer, W.; Marais, G.; Matsuo, T. Activated Sludge Model No. 1. *IAWPRC Sci. Tech. Reports* **1987**, *1*.

7. Valverde-Pérez, B.; Mauricio-Iglesias, M.; Sin, G. Modelling and Control Design for SHARON / Anammox Reactor Sequence. In Proceedings of the Proceedings of the 17th Nordic Process Control Workshop; 2012.

8. Valverde-Pérez, B.; Mauricio-Iglesias, M.; Sin, G. Systematic Design of an Optimal Control System for the SHARON-Anammox Process. *J. Process Control* **2016**, doi:10.1016/j.jprocont.2015.12.009.

9. Iacopozzi, I.; Innocenti, V.; Marsili-Libelli, S.; Giusti, E. A Modified Activated Sludge Model No. 3 (ASM3) with Two-Step Nitrification-Denitrification. *Environ. Model. Softw.* **2007**, doi:10.1016/j.envsoft.2006.05.009.

10. Henze, M.; Gujer, W.; Mino, T.; Loosdrecht, M. van Activated Sludge Models AS. **2000**.

11. Bozkurt, H.; Quaglia, A.; Gernaey, K. V; Sin, G. Environmental Modelling & Software A Mathematical Programming Framework for Early Stage Design of Wastewater Treatment Plants. *Environ. Model. Softw.* **2015**, *64*, 164–176, doi:10.1016/j.envsoft.2014.11.023.

12. Ostace, G.S.; Cristea, V.M.; Agachi, P.Ş. Cost Reduction of the Wastewater Treatment Plant Operation by MPC Based on Modified ASM1 with Two-Step Nitrification/Denitrification Model. *Comput. Chem. Eng.* **2011**, *35*, 2469–2479, doi:10.1016/j.compchemeng.2011.03.031.

13. Giusti, E.; Marsili-libelli, S.; Spagni, A. Environmental Modelling & Software Modelling Microbial Population Dynamics in Nitritation Processes. *Environ. Model. Softw.* **2011**, *26*, 938–949, doi:10.1016/j.envsoft.2011.02.001.

14. Montgomery, D.C.; Runger, G.C.; Hubele, N.F. *Engineering Statistics*; 2011;

15. COST European Cooperation of Scientific and Technical Research *The COST Simulation Benchmark: Description and Simulator Manual*; 1998;

16. Kim, M.; Rao, A.S.; Yoo, C. Dual Optimization Strategy for N and P Removal in a Biological Wastewater Treatment Plant. *Ind. Eng. Chem. Res.* **2009**, *48*, 6363–6371, doi:10.1021/ie801689t.

17. Guerrero, J.; Guisasola, A.; Vilanova, R.; Baeza, J.A. Improving the Performance of a WWTP Control System by Model-Based Setpoint Optimisation. *Environ. Model. Softw.* **2011**, *26*, 492–497, doi:10.1016/j.envsoft.2010.10.012.

18. Ostace, G.S.; Baeza, J.A.; Guerrero, J.; Guisasola, A.; Cristea, V.M.; Agachi, P.Ş.; Lafuente, J. Development and Economic Assessment of Different WWTP Control Strategies for Optimal Simultaneous Removal of Carbon, Nitrogen and Phosphorus. *Comput. Chem. Eng.* **2013**, *53*, 164–177, doi:10.1016/j.compchemeng.2013.03.007.

19. Frey, H.C.; Patil, S.R. Identification and Review of Sensitivity Analysis Methods. *Risk Anal.* **2002**, *22*, 553–578.

20. Hamby, D.M. A Review of Techniques for Parameter Sensitivity. *Environ. Monit. Assess.* **1994**, *32*, 135–154.

21. Benesty J., Chen J., Huang Y., C.I. Pearson Correlation Coefficient. In: Noise Reduction in Speech Processing. *Encycl. Syst. Biol.* **2009**.

22. Sin, G.; Gernaey, K. V.; Neumann, M.B.; van Loosdrecht, M.C.M.; Gujer, W. Global Sensitivity Analysis in Wastewater Treatment Plant Model Applications: Prioritizing Sources of Uncertainty. *Water Res.* **2011**, *45*, 639–651, doi:10.1016/j.watres.2010.08.025.

23. Sung, S.W.; Lee, J.; Lee, I.-B. *Process Identification and PID Control*; 2009;

24. Weijers, S.R.; Preisig, H.A. Robustness Analysis of Model Predictive Control of Activated Sludge Plants. *IFAC Proc. Vol.* **2000**, *33*, 545–550, doi:10.1016/s1474-6670(17)38597-x.

25. Tang, X.; Sun, Y.; Zhou, G.; Miao, F. Coordinated Control of Multi-Type Energy Storage for Wind Power Fluctuation Suppression. *Energies* **2017**, *10*, 1–17, doi:10.3390/en10081212.